ELSEVIER

Earth and Planetary Science Letters 208 (2003) 85–99

EPSL

www.elsevier.com/locate/epsl

$^{40}Ar/^{39}Ar$ dating of the Rajahmundry Traps, Eastern India and their relationship to the Deccan Traps

Kim B. Knight [a,b,*], Paul R. Renne [a,c], Angus Halkett [d], Nicky White [d]

[a] *Department of Earth and Planetary Science, University of California, Berkeley, CA 94720, USA*
[b] *Danish Lithosphere Center, Øster Voldgade 10, L, 1350 Copenhagen K, Denmark*
[c] *Berkeley Geochronology Center, 2455 Ridge Road, Berkeley, CA 94709, USA*
[d] *Bullard Laboratories, Madingley Rise, Madingley Road, Cambridge CB3 0EZ, UK*

Received 5 March 2002; received in revised form 31 October 2002; accepted 23 December 2002

Abstract

Rajahmundry lava flows exposed along India's eastern coast have long been suggested to be outliers of the more massive Deccan Traps despite the distance of more than 400 km separating their present-day erosional remnants. Recent rock quarries in Rajahmundry Trap lavas of basaltic composition have exposed fresh surfaces available for sampling displaying clear stratigraphic relationships within the typical basalt–sediment–basalt stratigraphy. $^{40}Ar/^{39}Ar$ ages for plagioclase separates from eight Rajahmundry lavas both above (Upper Trap) and below (Lower Trap) the continuous sedimentary interlayer reveal a mean age of 64.7 ± 0.5 Ma. Plagioclase Ca/K values are high (20–350), requiring use of finer grain sizes (63–125 μm) and well-known interference corrections for Ar isotopes produced during sample irradiation to produce the best possible ages. Individual ages confirm the rapid eruption (< 2 Myr) of the Upper and Lower Rajahmundry lavas. These data indicate a lengthy hiatus between volcanism and subsequent deposition of Eocene sandstones, which locally overly the Rajahmundry sequences. These age data also place the eruption of the Rajahmundry Traps coincident with late-stage Deccan Trap volcanism. This synchronicity is consistent with new geochemical data and published paleomagnetic evidence. An unequivocal temporal connection between the Rajahmundry Traps and Deccan Traps may necessitate revision of transport mechanisms of melt and/or flow distances in the Deccan Traps.

Keywords: Rajahmundry Traps; Deccan Traps; argon; geochronology; Cretaceous–Tertiary; flood basalt

1. Introduction

The Rajahmundry Trap lava flows of eastern peninsular India occupy ~35 km^2 centered on the Krishna–Godavari Basin, and extend ~70 km offshore in the subsurface (Fig. 1). Striking NE–WSW, these lava flows dip ~5° to the SE, towards the Bay of Bengal. Their total extent in the subsurface is ~15 000 km^2, with a thickness ranging up to 150 m [1]. Despite lying ~400 km east of the nearest outcrop of Deccan Trap basalt, the Rajahmundry Traps have long been speculated to be outliers of the more extensive and

* Corresponding author. Tel.: +1-510-643-4466; Fax: +1-510-643-9980.
E-mail address: kbk@uclink.berkeley.edu (K.B. Knight).

0012-821X/03/$ – see front matter
doi:10.1016/S0012-821X(02)01154-8

better studied Deccan Trap flood basalts [2,3,4], the bulk of which were erupted near the Cretaceous–Tertiary (K–T) boundary (ca. 65.5 Ma; see [5] and references therein). Erosional remnants of the Deccan Traps cover a present-day area exceeding 5×10^5 km^2 across western central India (Fig. 1) and are plausible contributors to the massive biotic changes occurring at the end of the Cretaceous [6]. The pre-erosional expanse of the Deccan Traps, however, remains speculative and there is a lack of physical data documenting the extent of individual flows within the province. Here, we further explore the temporal and possibly spatial connection between the Rajahmundry Traps and Deccan Traps through application of $^{40}Ar/^{39}Ar$ dating to mineral separates from the Rajahmundry lava flows. These data bear directly on our understanding of the timing and evolution of the Deccan Traps, as well as magma generation, storage and transport processes in continental flood basalt provinces, as a whole.

Rajahmundry lava flows display a well-established stratigraphy (Fig. 2), generally underlain by series of Late Cretaceous limestones, and overlain by the Rajahmundry Sandstone of Eocene age. Onshore, exposures of Rajahmundry Trap lava flows average $\sim$60 m in thickness including a laterally continuous sedimentary interlayer of limestone and shale ($\sim$2 m thick, total) overlying lateritized basalt. This sedimentary interlayer, separating the Lower Traps from the Upper Traps, indicates a hiatus in lava flow emplacement of unknown duration. The offshore sequence (sometimes referred to as the Razole Formation) often contains series of thin interbedded sediments between multiple flows, with a more prominent sedimentary unit representing the hiatus between Upper and Lower Trap flows [7]. The exact number of lava flows within the Rajahmundry Traps remains unclear due to limited exposure and mapping, but the generalized basalt–sediment–basalt stratigraphy defining the Lower Trap flows from those of the Upper Traps is found in all sections used in this study. Additional morphological detail on Rajahmundry Trap flows can be found in [8].

Onshore, preserved lava flows are rarely fresh where exposed at natural outcrops, a result of an intensive weathering environment. Use of the Rajahmundry Trap basalt as local building material, however, has recently exposed fresh lava flows in several local quarries (Fig. 1). As well as making fresh materials available for study, these quarries permit stratigraphic relationships to be more clearly established. Rajahmundry Trap samples used for this study were collected in quarries exposing subaerially erupted lava flows. Compositionally, these lava flows are basalts with holocrystalline textures. Rare phenocrysts of olivine (usually altered except in the freshest samples), clinopyroxene and plagioclase laths are present. Plagioclase phenocrysts commonly contain inclusions, including apatite, and display optical zoning that reflects compositional variation from core to rim. Ti-magnetite and ilmenite are also present, often making up more than 5% of the bulk rock mass.

The SiO_2 and alkali (K_2O+Na_2O) contents of these lava flows range from 48.5 to 51.0% and from 2.1 to 2.9%, respectively (Table 1), typical of subalkaline basalts. High TiO_2 contents (2.0–2.9%) for subalkaline compositions suggest a high-Ti tholeiitic basalt magmatic composition. The Rajahmundry Trap flows are relatively enriched in Fe ($\sim$13% total Fe expressed as FeO), broadly similar to younger Deccan Trap formations (Fig. 3) such as the Ambenali, Poladpur and Mahabaleshwar formations (Table 1), which are defined largely on the basis of geochemical and stratigraphic data (e.g. [9]).

The set of six analyses reported here shows two statistically separate groups of lavas within the Rajahmundry Traps which *do not* reflect the division of 'Upper Traps' and 'Lower Traps'. Samples RA99.1B, .06 and .12 are more enriched in CaO with correspondingly lower K_2O contents than samples RA99.02, .14 and .23. This division is also reflected in a simple SiO_2 vs. MgO diagram, more primitive samples being those with higher wt% CaO. The sample RA99.12 from the Lower Trap flows is distinctive as the most primitive sample analyzed with 7.3% MgO, as well as having the lowest wt% TiO_2 and total Fe of the suite.

Trace element data (Table 1), when normalized to primitive mantle [10], show slight depletion of more mobile trace elements (Rb, Ba), most prob-

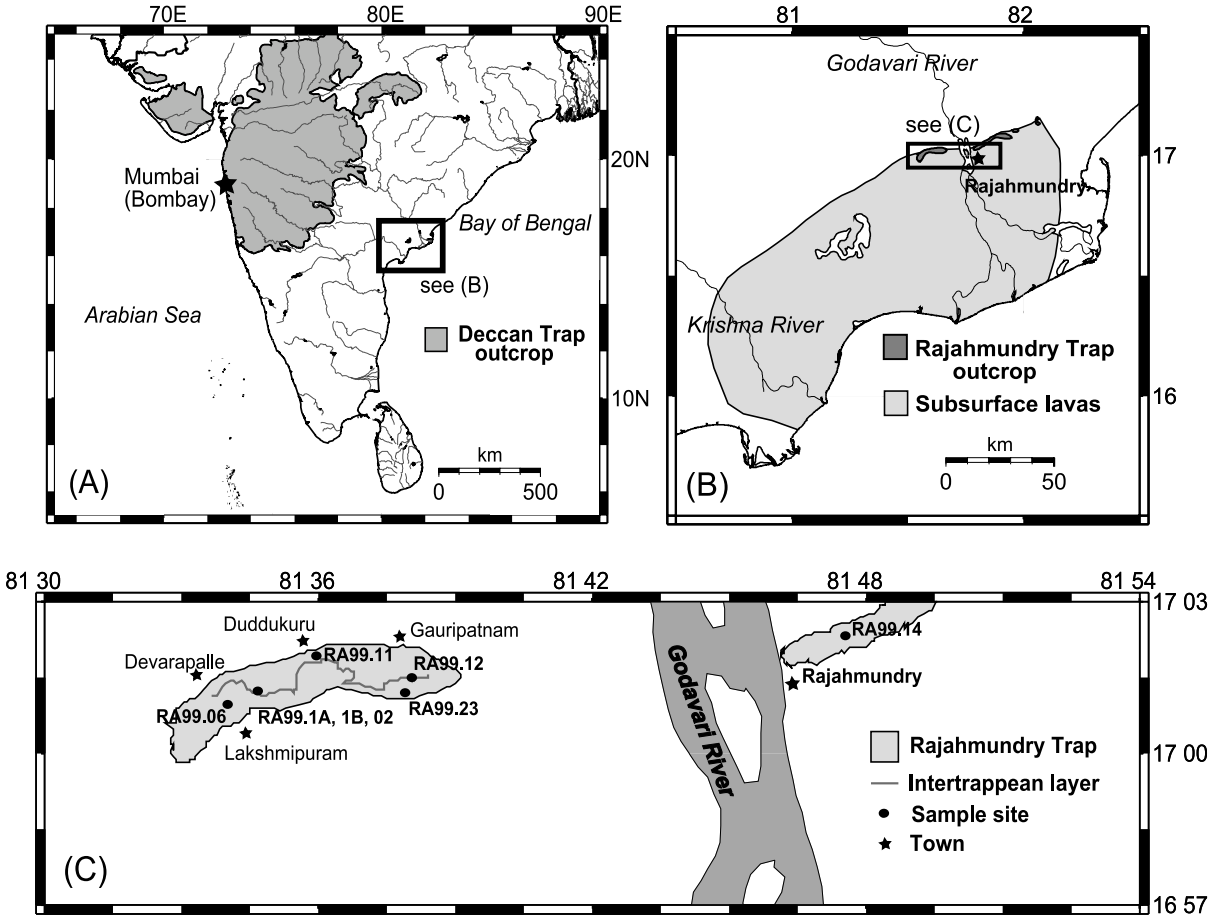

Fig. 1. (A) The present-day extent of the Deccan Traps. (B) Known surface outcrops and the subsurface extent of the Rajahmundry Traps after [1]. (C) The onshore exposures of the Rajahmundry Traps and site locations of samples used in this study.

ably a result of mild alteration. All samples show light enrichment of the light rare earth elements normalized to chondritic abundances [11] (La/Sm ~ 1.4) and no notable Eu anomaly (Fig. 4). Sample RA99.12, while sharing the same generalized trace element characteristics as all other samples presented here, as well as those reported in [12], has relatively depressed values. Geochemical analyses from [13] are not considered representative, as discussed and summarized in [12], and are not used here for comparative purposes.

The Rajahmundry Traps are preserved between Late Cretaceous limestone and Eocene-aged sandstone. Three ONGC (Oil and Natural Gas Corporation) wells drilled through the Rajahmundry sequence contain paleontological microfossils preserved in both the underlying and interlayered sediments, reportedly constraining volcanism to between 68 and 60 Ma [7]. Closer study of one of these wells failed to precisely locate the K–T transition, but convincingly places the interlayered sediments within an early Danian (post K–T) timeframe based on foraminiferal evidence [14]. These paleontological data, however, shed little light on the absolute age of the entire Rajahmundry Trap sequence, as their use as a measure of the timing and duration of the Rajahmundry Trap volcanism is strongly dependent on calibration of the geologic time scale for the taxa used.

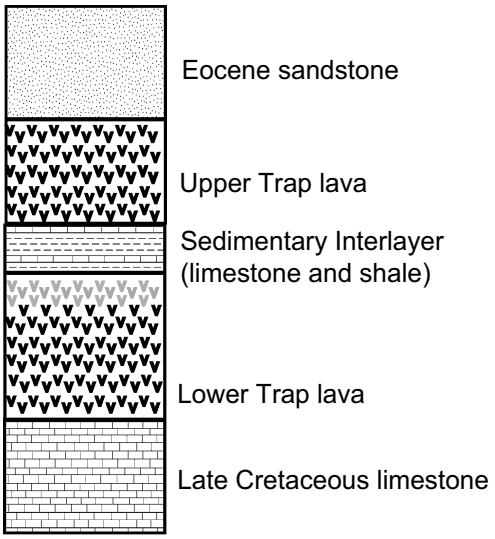

Fig. 2. Generalized onshore stratigraphy (not to scale) for the Rajahmundry Traps.

Paleomagnetic studies have long inferred that the Rajahmundry Traps were wholly of normal polarity [15,16]. In 1992, however, the occurrence of reversed polarity lava within the Rajahmundry sequence was reported as part of a larger study of the Deccan Traps [17]. Two samples from the Upper Traps revealed normal polarity, while a flow with reversed polarity was contained in the Lower Traps. The polarity reversal was identified as C29r–C29n on the basis of paleontological data and modeled eruption rates. The occurrence of reversely magnetized flows within the Lower Traps of Rajahmundry has since been observed by several authors (e.g. [13] – see comment [18] and reply [19]). The precise stratigraphic location of the reverse to normal boundary within the Rajahmundry Trap lava flows, however, remains unmapped and it is unclear if the boundary in magnetic polarity occurs above or below the interlayered sediments. The C29r–C29n paleomagnetic stratigraphy associates the Rajahmundry lava flows with the same reverse to normal transition observed in late-stage Deccan Trap volcanism (Fig. 8) (see [20] for a review).

This study focuses on dating of fresh plagioclase separates from eight different sites above and below the sedimentary interlayer (i.e. plagioclase from both Upper Trap and Lower Trap lava flows) of the Rajahmundry Traps. Initial $^{40}Ar/^{39}Ar$ dating of the Rajahmundry Traps [4] performed on two whole rock samples taken from above and below the sedimentary interlayer yielded ages (normalized to Fish Canyon sanidine at 28.02 Ma) of 64.4 ± 1.0 Ma and 63.9 ± 0.8 Ma (at the 2σ level). More recent replicates of these whole rock samples [12] yielded ages of 64.5 ± 0.3 and 64.0 ± 0.4 (taken from normalized weighted means of each sample's replicate analyses). Several of these whole rock samples, each heated in six or seven steps, show obvious problems, including signs of recoil. Recoil occurs when ^{39}Ar is generated in the $^{39}K(n,p)^{39}Ar$ reaction with sufficient excess energy to cause redistribution or loss of the ^{39}Ar. If the distribution of reactor-induced ^{39}Ar varies from the original distribution of ^{39}K in the sample, the incremental release with increasing temperature of the ^{39}Ar gas, as well as the resulting plateau, will vary according to the Ar retentivity of the material with implanted ^{39}Ar. $^{40}Ar/^{39}Ar$ dating of whole rock samples is susceptible to problems associated with ^{39}Ar recoil [21], particularly in the presence of alteration, a common feature of Rajahmundry Trap lava flows [8] as well as Deccan Trap lava flows [5]. Analyses of fresh plagioclase separates with large grain size compared to recoil dimensions are expected to yield more reliable $^{40}Ar/^{39}Ar$ ages since they are free from visible alteration and less prone to recoil loss or redistribution of Ar. This study marks the first single phase dating of Rajahmundry Trap lavas.

2. Methodology

Fresh hand samples taken from outcrops exposed in quarries were crushed in tungsten carbide mills and separated into sieved size fractions. Plagioclase was isolated through use of a Frantz magnetic separator. Plagioclase separates were then cleaned in dilute nitric acid and hand-picked for irradiation. The preferred size fraction (eight samples) was 63–125 μm, minimizing the presence of inclusions and alteration, both common features of Rajahmundry Traps plagioclase. In four cases 125–425 μm size fractions of plagioclase

Table 1
Major (wt% oxide) and trace element (ppm) data for selected Rajahmundry Trap samples

		RA99.1B lower	RA99.06 upper	RA99.12 lower	RA99.23 upper	RA99.14 upper	RA99.02 lower	Panhala formation	Mahab.[a] formation	Kolhapur unit	Ambenali formation	Poladpur formation
SiO_2	XRF	48.50	49.17	49.24	50.10	50.33	50.95	49.75	49.40	48.92	49.28	50.23
Al_2O_3	XRF	14.15	14.35	14.61	12.93	13.02	13.43	14.80	13.60	13.36	13.72	13.68
TiO_2	XRF	2.64	2.59	1.98	2.80	2.85	2.76	1.83	2.98	3.02	2.61	2.19
FeO*	XRF	13.46	12.08	11.71	14.78	13.98	13.82	12.30	13.24	13.02	13.69	12.57
MnO	XRF	0.19	0.17	0.18	0.24	0.25	0.24	0.19	0.21	0.23	0.21	0.20
CaO	XRF	11.30	11.57	11.50	10.08	10.36	10.30	11.13	10.46	10.33	10.88	10.46
MgO	XRF	6.26	6.43	7.32	5.67	5.81	5.45	5.83	5.87	5.83	6.28	6.55
K_2O	XRF	0.12	0.10	0.09	0.39	0.36	0.41	0.41	0.38	0.32	0.27	0.37
Na_2O	XRF	2.28	2.20	2.04	2.36	2.37	2.50	2.49	2.46	2.47	2.33	2.45
P_2O_5	XRF	0.23	0.22	0.16	0.26	0.27	0.27	0.19	0.28	0.39	0.24	0.21
Total		99.13	98.89	98.83	99.62	99.59	100.12					
Ni	XRF	79	85	100	60	58	59	73	86	72	90	101
Cr	XRF	179	197	204	81	77	80	93	144	139	148	197
V	XRF	400	392	362	451	443	439	335	443	397	447	400
Ga	XRF	26	24	21	22	22	23	21	23	–	24	23
Cu	XRF	217	206	158	243	221	237	171	226	264	215	184
Zn	XRF	116	109	96	130	133	130	98	117	124	114	101
La	ICP-MS	13.2	12.4	7.8	15.0	15.6	15.9	14.6	15.1	16.7	11.8	13.5
Ce	ICP-MS	29.7	28.3	18.4	33.5	34.5	34.7	33.8	36.3	41.7	27.2	31.1
Pr	ICP-MS	4.0	3.9	2.6	4.5	4.6	4.7	–	–	–	–	–
Nd	ICP-MS	19.6	18.7	13.2	21.6	21.6	22.3	18.6	23.5	27.2	20.4	19.7
Sm	ICP-MS	6.0	5.7	4.3	6.4	6.6	6.7	4.5	6.1	7.3	5.7	5.5
Eu	ICP-MS	2.1	2.0	1.6	2.1	2.2	2.2	1.4	2.0	2.4	2.0	1.8
Gd	ICP-MS	6.7	6.5	5.1	7.1	7.3	7.5	–	–	–	–	–
Tb	ICP-MS	1.1	1.1	0.9	1.2	1.3	1.3	1.1	1.2	–	1.1	1.1
Dy	ICP-MS	6.8	6.5	5.2	7.5	7.7	7.7	–	–	–	–	–
Ho	ICP-MS	1.3	1.3	1.0	1.5	1.5	1.5	–	–	–	–	–
Er	ICP-MS	3.4	3.2	2.6	3.9	4.1	4.1	–	–	–	–	–
Tm	ICP-MS	0.5	0.4	0.4	0.5	0.6	0.6	–	–	–	–	–
Yb	ICP-MS	2.7	2.6	2.0	3.3	3.3	3.3	2.6	3.1	3.7	3.0	2.8
Lu	ICP-MS	0.40	0.38	0.31	0.49	0.50	0.51	0.40	0.49	0.58	0.48	0.44
Ba	ICP-MS	59	48	44	147	164	194	104	131	179	56	123
Th	ICP-MS	1.4	1.4	0.9	1.9	1.9	1.9	2.2	1.9	2.3	1.3	2.2
Nb	ICP-MS	13.2	12.8	6.8	12.9	13.3	12.9	9.8	16.6	16.8	10.9	9.5
Y	ICP-MS	33.8	32.3	26.2	39.1	40.0	40.0	32.2	37.5	41.8	35.1	34.8
Hf	ICP-MS	4.0	3.9	2.9	4.6	4.7	4.7	3.1	4.2	5.2	4.0	3.7
Ta	ICP-MS	0.9	0.9	0.5	0.9	0.9	0.9	0.8	1.0	1.3	0.8	0.7
U	ICP-MS	0.4	0.3	0.2	0.4	0.4	0.5	–	–	–	–	–
Pb	ICP-MS	1.3	1.2	1.2	2.5	2.7	2.7	–	–	–	–	–
Rb	ICP-MS	1.3	0.4	0.8	5.1	5.9	11.6	10.4	9.4	12.7	6.1	10.1
Cs	ICP-MS	0.02	0.00	0.02	0.05	0.07	0.18	–	–	–	–	–
Sr	ICP-MS	247	258	229	216	231	222	213	244	230	215	221
Sc	ICP-MS	41	41	41	45	46	46	–	–	–	36	36
Zr	ICP-MS	145	140	100	164	167	164	126	174	193	151	143

Averages of published geochemical data from several late-stage Deccan Trap formations [9,32–37] are presented for general comparison only. A dashed line indicates no available data. Total Fe expressed as FeO. Samples analyzed by X-ray fluorescence (XRF) and inductively coupled plasma mass spectrometry (ICP-MS), as noted, at Washington State University. Technical notes and descriptions of analytical procedures can be found at http://www.wsu.edu/~geology/Pages/Services/Geolab.html and are available on request.

[a] Mahab. = Mahabaleshwar.

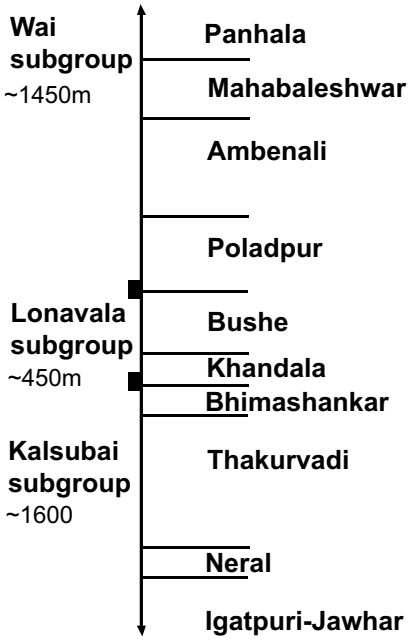

Fig. 3. Generalized stratigraphy of geochemical formations of the Deccan Traps after [27] and references therein. Formations are scaled to show relative maximum thickness. Maximum thickness of combined western Deccan Trap formations may be >3500 m.

were also hand-picked for analysis. Following selection, a total of 12 samples along with bracketing standards of Fish Canyon sanidine with an age of 28.02 ± 0.32 Ma [22] were loaded into two aluminum disks and co-irradiated for 7 h using the cadmium-lined in-core irradiation tube (CLICIT) facility of the Oregon State University TRIGA reactor.

All standards and samples were analyzed at the Berkeley Geochronology Center. Standards were analyzed as single grains using a CO_2 laser. Total variance of the neutron fluence as calculated for both disks was ≤0.35%. Bulk plagioclase samples were degassed incrementally with a CO_2 laser using an integrator lens to provide uniform heating over 0.5 cm wells in a copper disk, and analyzed using a MAP 215C mass spectrometer. Samples were degassed using 20–23 temperature steps, depending on individual sample behavior. Data corrected for backgrounds, mass discrimination and radioactive decay are available (see table 1 in the **Background Data Set**[1]). Analyses of 51 air pipettes (sampling atmospheric argon) were used to correct samples for mass discrimination (typically 1.006 ± 0.002 per atomic mass unit). The mean and standard deviation of background argon isotope abundances are shown in Table 2, along with the range of abundances for samples, which were generally well above the background levels.

Plagioclase separates from the Rajahmundry Traps frequently display very high Ca/K ratios (up to ~350), making corrections for the reactor-induced reaction $^{40}Ca(n,n\alpha)^{36}Ar$ substantial. When applying the $^{40}Ar/^{39}Ar$ method of dating, the $^{40}Ar/^{36}Ar$ ratio of samples is measured and compared with the $^{40}Ar/^{36}Ar$ ratio of atmosphere (~296) in order to correct ^{40}Ar (as measured in the samples) for the additional contribution of atmospheric argon. Application of this atmospheric correction assumes that ^{36}Ar present in the sample is a result of equilibration of the sample with atmospheric Ar. The extreme Ca/K ratio in several Rajahmundry Trap samples makes knowledge of the reactor-induced $^{36}Ar_{Ca}$ production essential in order to correct measured ^{36}Ar for the contribution not attributable to atmospheric Ar. Compiled data from 11 irradiations of CaF_2 salts at the TRIGA facility over the past decade, summarized by [22], were used to determine a mean $(^{36}Ar/^{37}Ar)_{Ca}$ production ratio of $(2.67 \pm 0.14) \times 10^{-4}$ (2σ).

3. $^{40}Ar/^{39}Ar$ results

CO_2 laser incremental heating analyses of 12 plagioclase separates from Rajahmundry Trap lava flows reveals a weighted mean age for the eight samples (12 analyses, total) achieving plateaux of 64.7 ± 0.5 Ma (including the error of the neutron fluence monitor). Plateaux are herein defined as the release of 50% or greater of the total ^{39}Ar gas released in five or more successive steps concordant within 2σ error and showing no resolvable slope. Plateaux were achieved for all analyzed samples (Figs. 3 and 4). Slight Ar loss

[1] http://www.elsevier.com/locate/epsl

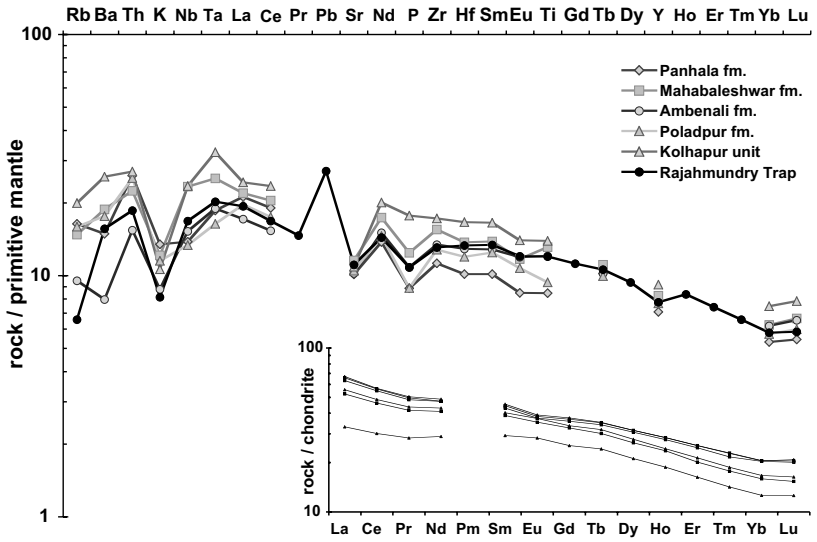

Fig. 4. Averaged trace element data (Table 1) for six Rajahmundry Trap samples shown normalized to primitive mantle [10], listed in order of compatibility. Average values from available data [9,32–37] for the Panhala, Mahabaleshwar, Ambenali and Poladpur formations of the Deccan Traps, as well as the Kolhapur unit of the Mahabaleshwar Formation are shown for comparison. Inset shows rare earth element data normalized to chondrite [11] for individual Rajahmundry Trap samples. Circles indicate Lower Trap lavas, squares indicate Upper Trap lavas.

likely due to small amounts of alteration is present in all age spectra at the lowest temperature steps. All replicate analyses, regardless of grain size fraction analyzed, are concordant at the 2σ level. Age errors are reported at the 2σ level and exclude contributions from systematic sources [22,24] as all age comparisons made herein concern $^{40}Ar/^{39}Ar$ ages normalized to the same standard basis. Mean square of weighted deviates (MSWD) values range from 0.3 to 1.6, indicating generally good correspondence between expected errors and estimated errors. A majority of values < 1 suggests overestimation of analytical errors in several cases, possibly the result of unrecognized correlation between sources of error. Results of individual analyses are summarized in Table 3.

Spectra from eight analyses of five samples of Lower Trap basalts (Fig. 5) give plateau ages with a weighted mean age of 65.0 ± 1.1 Ma at the 95% confidence level. Sample RA99.11 displays gently

Table 2
Background and sample gas yields (in mol) from analytical data

	Abundances (mol)				
	^{40}Ar	^{39}Ar	^{38}Ar	^{37}Ar	^{36}Ar
Average (background)	7.80E−17	1.17E−18	2.03E−19	2.74E−18	5.45E−19
1σ	1.55E−17	2.42E−19	1.07E−19	1.00E−18	1.42E−19
Maximum (sample)	8.54E−14	9.80E−16	5.38E−17	2.69E−14	2.80E−16
Minimum (sample)	3.56E−16	7.04E−18	1.74E−19	3.13E−16	7.25E−19
Average (sample)	8.63E−15	1.79E−16	5.61E−18	8.44E−15	1.98E−17
1σ	1.31E−14	1.94E−16	8.18E−18	5.90E−15	3.90E−17

Averaged data and standard deviation from 115 background analyses are shown to characterize backgrounds. Maximum, minimum and average values from step heating of unknowns resulting in a contribution of 0.5% or greater release of ^{39}Ar gas to total gas analyzed are shown to characterize samples. Gas yields (in mol) are computed from amplified ion beam currents using air pipette volume estimates.

Table 3
$^{40}Ar/^{39}Ar$ age summary for plagioclase separates from Rajahmundry Trap lava flows

Sample	Grain size analyzed (μm)	Lava group	Plateau age (Ma)	MSWD	^{39}Ar (% of total)	Isochron age (Ma)	$^{40}Ar/^{36}Ar$ intercept	Average Ca/K
RA99.1A	125–425	lower	66.0 ± 2.9	0.5	59.1	67 ± 4	295 ± 6	331
RA99.1B	63–125	lower	65.0 ± 1.6	0.6	98.9	67 ± 2	287 ± 12	205
RA99.1B(a)	125–425	lower	62.7 ± 2.3	0.3	73.9	40 ± 30	380 ± 130	353
RA99.1B(b)	125–425	lower	65.3 ± 1.9	0.4	89.9	69 ± 4	280 ± 15	343
RA99.02	63–125	lower	65.8 ± 0.5	0.6	81.9	65.2 ± 0.5	297 ± 1	20
RA99.06	125–425	upper	64.6 ± 1.9	0.3	87.7	64 ± 3	300 ± 30	302
RA99.06	63–125	upper	63.5 ± 1.1	0.4	88.5	61.8 ± 1.3	299 ± 3	123
RA99.11	63–125	lower	63.7 ± 0.8	0.1	76.4	63.7 ± 1.2	296 ± 17	115
RA99.12(a)	63–125	lower	64.6 ± 0.8	0.3	86.7	65.0 ± 0.9	286 ± 20	105
RA99.12(b)	63–125	lower	64.8 ± 0.8	1.1	87.9	62.7 ± 2.0	350 ± 50	99
RA99.14	63–125	upper	64.3 ± 0.4	1.6	75.2	64.5 ± 0.4	280 ± 20	24
RA99.23	63–125	upper	64.7 ± 0.4	0.5	87.2	64.8 ± 0.3	289 ± 19	25

Errors shown are internal errors and reflect uncertainties in isotope measurements, corrections for reactor-induced interference and neutron fluence (J).
Ages calculated using the following decay constants: $\lambda(^{40}K)_{ec} = 5.81\times10^{-11} \pm 3.4\times10^{-12}$ yr^{-1} (value from [47] using errors from [24]), $\lambda(^{40}K)_{\beta} = 4.96\times10^{-10} \pm 1.7\times10^{-11}$ yr^{-1} [48], $\lambda(^{37}Ar) = 1.983\times10^{-2} \pm 4.4\times10^{-5}$ d^{-1} [23]. Correction factors for the OSU TRIGA reactor are: $(^{36}Ar/^{37}Ar)_{Ca} = 2.67\times10^{-4} \pm 1.4\times10^{-5}$, $(^{39}Ar/^{37}Ar)_{Ca} = 6.95\times10^{-4} \pm 1.8\times10^{-5}$, $(^{40}Ar/^{39}Ar)_{K} = 7.3\times10^{-4} \pm 1.8\times10^{-5}$ from [22] and unpublished data. All errors shown at 2σ.

disturbed spectra and falls outside of this mean age, but cannot be considered to be significantly younger. Sample RA99.02 (65.8 ± 0.5 Ma) yields an apparent age plateau significantly older than and statistically distinct from the mean age for the Lower Traps. This sample's age spectrum, whose precise plateau age is occasioned by a low Ca/K ratio of ~20, shows significant discordance consistent with the presence of excess argon in higher temperature steps. In view of the obvious discordance, which is clearly not an analytical artifact, we cannot be confident that the plateau age – despite being defined by relatively rigorous objective criteria – is unbiased. Consequently, we conclude that the plateau 'age' for this sample may not be meaningfully interpretable. Samples RA99.1A, one analysis of RA99.1B and RA99.02, while achieving plateaux, clearly show disturbed spectra at the highest temperature steps well outside of 2σ error. In addition, sample RA99.12(b) yields an isochron age just outside of error of the plateau age, and an $^{40}Ar/^{36}Ar$ intercept just beyond that of atmosphere. This sample also displays slight high temperature disturbance, though to a lesser degree than those previously discussed, and remains concordant with replicate analyses RA99.12(a), well within error.

The anomalously old apparent ages in high-temperature steps, as seen in several samples, are manifest in relatively large gas fractions, well beyond analytical blanks, and there is little likelihood that they are analytical artifacts. We tentatively infer that these anomalies reflect excess ^{40}Ar hosted in melt inclusions, as observed by Esser et al. [25], although in the Rajahmundry Trap plagioclase samples the anomalous ages are not consistently correlated with compositional anomalies involving K, Ca, or Cl. Anomalies such as these are more likely to become apparent using step heating of single mineral phases in place of degassing of whole rock material, which could obscure this level of detail and the presence of excess argon. Further discussion of excess argon and the effects of melt inclusions can be found in [26].

All four analyses from three samples of Upper Trap lava flows (Fig. 6) also yield plateau ages, all statistically indistinguishable within error. The weighted mean age of the Upper Traps is 64.5 ± 0.8 at the 95% confidence level, slightly

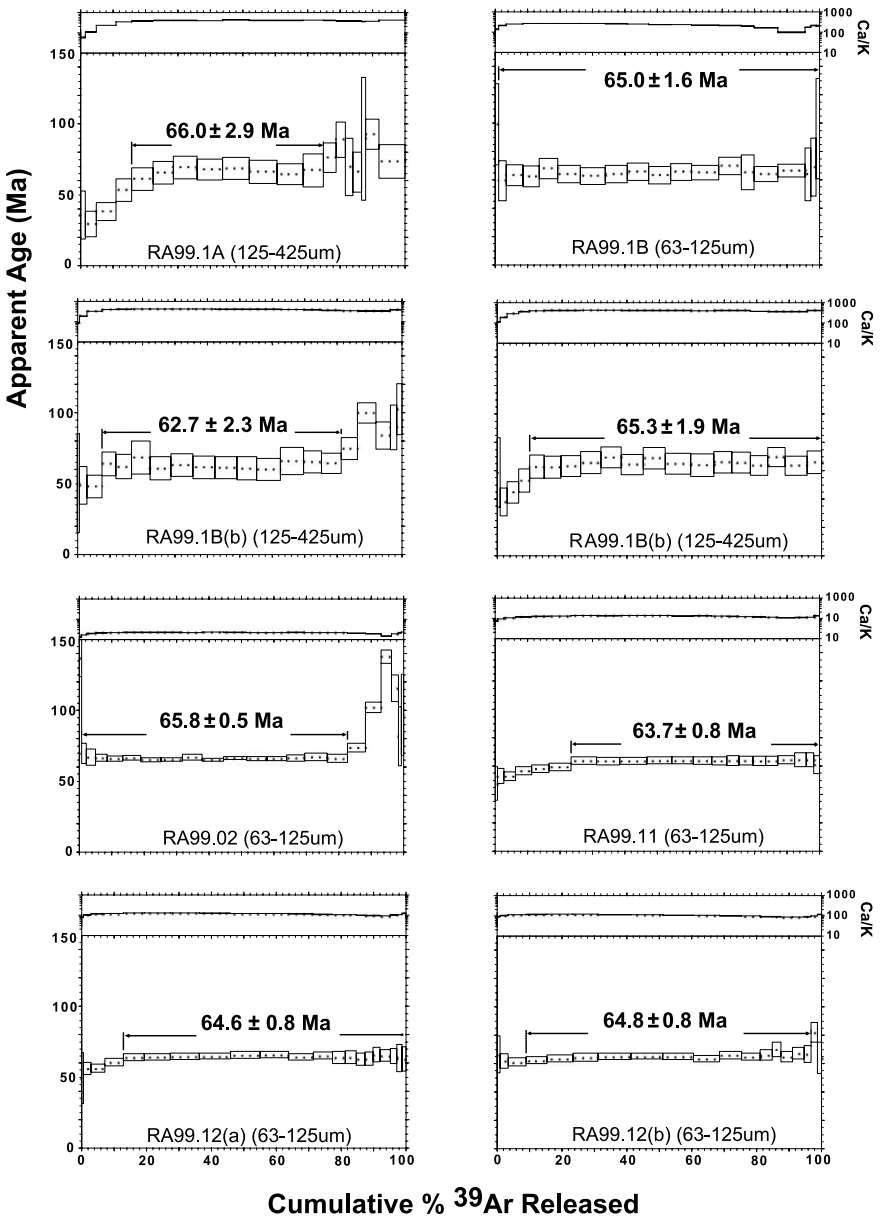

Fig. 5. $^{40}Ar/^{39}Ar$ apparent age spectra and Ca/K ratios from step heating of plagioclase separates from Lower Trap Rajahmundry lavas. Plateau ages with 2σ uncertainties (including uncertainty from isotope measurements, corrections, and neutron fluence) are shown.

younger than, but not distinguishable outside of error, of the weighted mean age for the Lower Traps. Replicate analyses of sample RA99.06 using two different size fractions of plagioclase provide the same age well within respective errors, despite the finer grain size displaying some slight disturbance in the higher temperature steps. The remaining two Upper Trap samples, RA99.14 and RA99.23, give identical plateau ages within error.

Extremely high Ca/K ratios (up to ~400) in

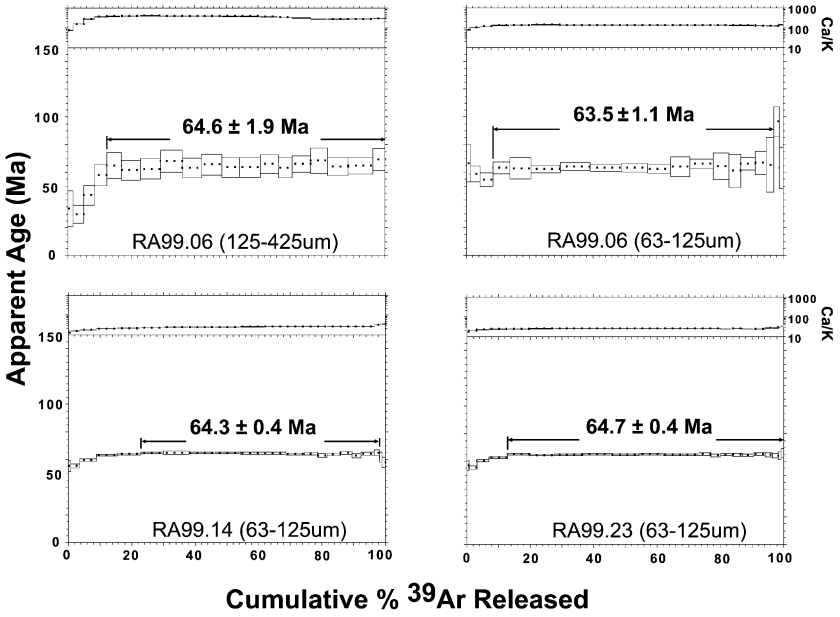

Fig. 6. $^{40}Ar/^{39}Ar$ apparent age spectra and Ca/K ratios from step heating of plagioclase separates from Upper Trap Rajahmundry basalts. Plateau ages with 2σ uncertainties (including uncertainty from isotope measurements, corrections, and neutron fluence) are shown.

several samples limit precision due to error propagation attending the large correction necessary for reactor-produced $(^{36}Ar)_{Ca}$. All four samples with larger grain size (125–425 μm versus 63–125 μm) display the highest Ca/K ratios of any samples analyzed (>300). This effect is clearly a result of proportionately higher concentration of more calcic phenocryst cores in the coarser fractions. Finer-grained separates of plagioclase from given lavas display lower Ca/K and thus higher precision (Fig. 7). In two cases (samples RA99.1B and RA99.06) replicate analyses of both a larger (125–425 μm) and smaller (63–125 μm) sieve fraction were analyzed. While in both cases determined $^{40}Ar/^{39}Ar$ ages of the same sample overlap at the 2σ level, errors for the larger size fractions increase, scaling with the massive $^{36}Ar_{Ca}$ correction. Excellent plateau ages as precise as 64.7 ± 0.4 and 64.6 ± 0.8 from above and below the sedimentary interlayer have been obtained from samples with relatively low Ca/K ratios (<50). No resultant bias in apparent ages corrected for $^{36}Ar_{Ca}$ is evident (Fig. 7). These results underscore the advantage of analyzing plagioclase fractions that may be significantly smaller than maximum phenocryst dimensions. Though generally more work is required to separate finer fractions, the dividend in data quality attending reduced Ca/K values is clear.

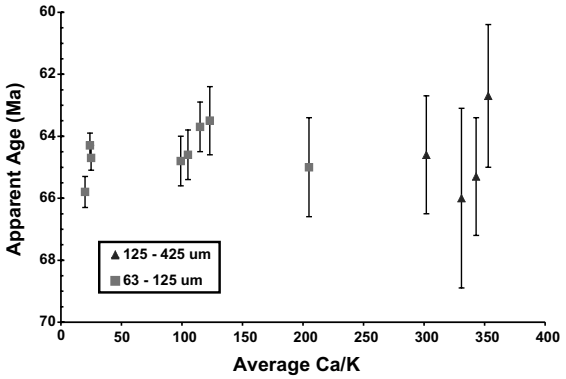

Fig. 7. A comparison between Ca/K ratio and apparent sample age. Triangle symbols indicate samples analyzed using the larger grain size (125–425 μm), square symbols indicate the finer grain size (63–125 μm). Note that a wide range of Ca/K ratios is represented in both the Upper and Lower Trap samples. There is no systematic bias in apparent sample age due to corrections made for Ca concentration beyond an increase in age uncertainty (shown here at 2σ).

4. Discussion

The $^{40}Ar/^{39}Ar$ ages from undisturbed spectra with both high and low Ca/K ratios indicate rapid (< 2 Myr) eruption (Fig. 8) of the entire Rajahmundry Trap sequence. These data clearly confirm a temporal correlation between the Rajahmundry Traps and late-stage Deccan Trap volcanism. Coincident emplacement of the Rajahmundry Traps may be the result of independent melt sources in relation to late-stage Deccan Trap volcanism, or may be the consequence of a petrogenetic relationship between the Rajahmundry Traps and the Deccan Traps. The main formations of the Deccan Traps, preserved as the Western Ghats, are mapped and classified on the basis of geochemical characterization [9]. This chemical stratigraphy (Fig. 3) has been enhanced and successfully applied to other regions of the Deccan Traps [27–31] to identify flow types (i.e. formations, not individual flows). Late-stage Deccan Trap formations comprise the Wai subgroup and include (oldest to youngest) Poladpur, Ambenali, Mahabaleshwar and Panhala formations (see [27] and references therein).

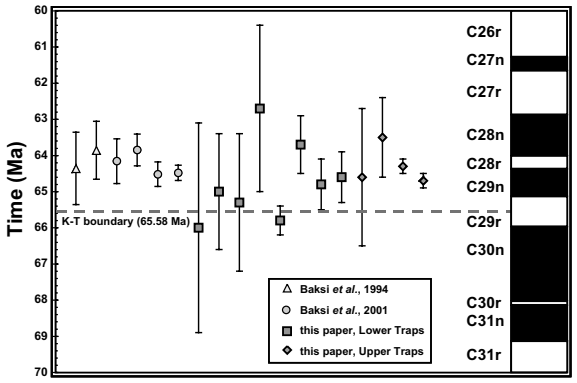

Fig. 8. Chronology of the Rajahmundry Traps. Magnetostratigraphy based on the time scale of [46]. Circles indicate sample $^{40}Ar/^{39}Ar$ ages for Upper Trap flows, whereas diamonds indicate Lower Trap flows (this study). Triangles represent $^{40}Ar/^{39}Ar$ data from [4], circles represent $^{40}Ar/^{39}Ar$ data from [12]. K–T boundary age (65.58 Ma) is shown by the dashed line. All represented data are shown calculated relative to the Fish Canyon sanidine standard at 28.02 Ma [22]. All errors reported at 2σ level.

Major element characteristics ($K_2O < 0.5\%$, $Na_2O > 2\%$ and $TiO_2 \sim 2$–3%) contents for Rajahmundry Trap lavas, as well as rare earth element concentrations, suggest a comparison between Rajahmundry Trap volcanism and late-stage Deccan Trap volcanism. Trace element data (especially rare earth element data) are sparse for Deccan Trap samples even along the better-studied western margin, allowing only generalized comparison at present. We performed a methodical comparison of trace element data from published data covering formations from the western margins and found the closest match of lavas from the Deccan Traps are the upper formations comprising the Wai subgroup of Deccan Traps (Fig. 4). Averages of published geochemical data from the Wai subgroup in the Western Ghats [9,32–37] are presented for comparison. A correlation specifically with the Kolhapur unit of the Mahabaleshwar Formation has been suggested [12], but published data on this unit (limited to [32]) and chemical variation within flows and formations (e.g. [9]) do not allow thorough evaluation of this claim.

Direct correlation of Rajahmundry and Deccan flows or flow units is difficult due to the paucity of studies along the eastern margin of preserved Deccan Trap volcanism, yet preliminary correlation can be explored. The portion of the Deccan Traps closest to the Rajahmundry Traps is exposed around the Godavari–Manjra and Penganga–Wardha River basins (Fig. 1), near the cities of Bidar and Nagpur. Limited mapping of this area [30] reports preserved volcanism dominated by Ambenali-like and Poladpur-like lavas, on the basis of major element geochemical classification, chemically similar to Rajahmundry Trap flows and supporting arguments for a petrogenetic as well as temporal relationship between the two volcanic events. Analytical comparison with trace element data recently available for northeastern Deccan Trap lavas [29,31], broadly associated with late-stage Deccan Trap volcanism, also displays similar geochemical characteristics as Rajahmundry Trap samples. While initial data seem permissible, studies of similar detail to those currently being undertaken within the Deccan Traps, particularly application of isotopic studies

to investigate source characteristics and characterize the nature and extent of crustal contamination, will better constrain petrogenetic arguments associating the Deccan Traps with the Rajahmundry Traps.

Overland flow of Deccan Trap lavas resulting in emplacement of the Rajahmundry Traps is one possible explanation for the temporally coincident occurrence of the two basalt provinces. Single flows in flood basalt provinces are known to flow distances of several hundred kilometers, such as the Pomona [38] and Ginkgo [39] flows of the Columbia River Flood Basalts. Exploration of the physical requirements for emplacement of long basaltic flows [40] suggests inflation of pahoehoe flows as a mechanism for large-scale flow of basaltic magma, and possibly as a primary mechanism for continental flood basalt emplacement. Recent reconstruction of the evolution of the SE-draining Krishna and Godavari River basins (both draining directly to the Rajahmundry area, Fig. 1) shows that these basins, draining much of the Indian Peninsula, existed and were active well before the formation of the main Deccan Traps [8]. Nonetheless, there are no published reports of remnant volcanism preserved within the Godavari and Krishna River channels. Moreover, individual flow distances on the order of 10^2 km are difficult to document or exclude in the Deccan Traps, due to the generally fine-grained nonunique texture and heavily weathered and/or vegetated state of most Deccan Trap flows. Although lavas sharing geochemical characteristics of certain formations (e.g. Poladpur and Ambenali formations) clearly occur throughout the bulk of the Deccan Traps, studies of isotope systematics from formations occurring in separated regions of the Deccan Traps [29,31] seem to indicate variable crustal contamination and localized eruption centers.

One further possibility for emplacement of the Rajahmundry Traps (again, implying a petrogenetic connection with the Deccan Traps) is the transport of melt via the upper crust. Upper crustal transport of melt feeding flows over distances of 1600 km has been inferred for the Ferrar Large Igneous Province (Antarctica) [41], Mackenzie dike swarm (Canada) [42], Karoo dikes (South Africa) [43] and the Botswana dike swarm associated with Karoo magmatism (southern Africa) [44]. In the Rajahmundry Traps there are no reported occurrences of dikes, feeder systems or sill-like structures which might lend credence to an hypothesis of subsurface melt transport. Searching for intrusive or feeder bodies is made more difficult as onshore lavas occupy a sedimentary basin, and the bulk of the Rajahmundry Traps are presently buried in offshore sediments. In the case of significant subsurface melt migration, one might expect to observe gravity or magnetic anomalies due to the cooling of the melt at shallow depth. Unfortunately, gravity and magnetic data for this region are sparse or unpublished, and not currently available for analysis. If significant subsurface melt transport could be substantiated, serious revision of the distribution and transport of melt in the Deccan Traps (as well as for large igneous provinces in general) would be necessary.

5. Conclusions

Radioisotopic age data from plagioclase separates presented in this study show that mean ages for both Upper Trap lava flows (64.5 ± 0.8 Ma) and Lower Trap lava flows (65.0 ± 1.1 Ma), while remaining stratigraphically consistent, are indistinguishable within error with a combined weighted mean age of 64.7 ± 0.5 Ma. Emplacement of the Rajahmundry Traps spans ~ 2 Myr at most using the 2σ error bars (Fig. 8) of plateau ages with lower Ca/K ratios (as discussed in the text) to bracket the duration of volcanism. Our data confirm the rapid emplacement of the Upper and Lower Rajahmundry Trap lava flows, and indicate a substantial hiatus between emplacement of the Upper Trap lava flows and the Eocene Rajahmundry Sandstone. Emplacement of the Rajahmundry Traps is coincident with late-stage Deccan volcanism and within ca. 1 Ma of initiation of main-stage Deccan volcanism in the Western Ghats (as discussed in [5]). Emplacement may slightly post-date the K–T boundary (65.6 ± 0.6 Ma as recalculated from [45] to the same standard calibration and decay constants used herein by

[22])[2]. Paleomagnetic studies [17] showing a reverse to normal magnetization polarity sequence within the Rajahmundry Traps support a temporal connection with waning Deccan Trap volcanism, consistent with our age results.

Our new data clearly imply a temporal connection between Rajahmundry Trap volcanism and late-stage Deccan Trap volcanism, but elucidation of the nature of this relationship remains in need of further study. Presently none of the above scenarios of independent melt generation, overland magma transport, or upper crustal flow of Deccan Trap-derived melt can be dismissed until further evidence is obtained. Rapid eruption of the Rajahmundry Trap volcanic sequence is evident, as well as a clear correlation between the Rajahmundry Traps and the Deccan Traps on the basis of age, remnant magnetization and general geochemistry. Further mapping of preserved volcanism around the little-studied eastern margins of the Deccan Traps, as well as documentation clarifying the presence or absence of possible erosional remnants of Rajahmundry Trap along the Godavari and Krishna River valleys, are needed to thoroughly address modes of emplacement for the Rajahmundry Traps. Supportable mechanisms for coincident emplacement of the Rajahmundry Trap lavas with late-stage Deccan Trap volcanism remain elusive, but, once established, may yet extend our estimates of the original extent of the Deccan Traps and provide new insight into melt generation and magma transport models relating to flood basalt provinces.

Acknowledgements

Mahesh Anand and the ONGC are thanked for their assistance. Bob Duncan is thanked for his thorough review and Sébastien Nomade for his helpful comments. We thank Mike Villeneuve for bringing to our attention the error in revising the age of the K–T boundary. The on-line GEOROC geochemical database provided by the Max-Planck-Institut für Chemie has been very much appreciated. This study was supported in part by the Danish Lithosphere Center (K.B.K.), the US National Science Foundation (Grant EAR-9909517 to P.R.R.) and NERC (A.H.). Earth Sciences Contribution Number 7214. ***[BOYLE]***

[2] Renne et al. [22] reported a recalculated age of 64.56 Ma for the K–T boundary but this age was based on an erroneous value of R_{FCs}^{IRZs}. The correct value (2.3496) yields an age of 65.46 Ma.

References

[1] D.S.N. Raju, B.C. Jaiprakash, A. Kumar, Palaeoenvironmental set-up and age of basin floor just prior to the spread of Deccan volcanism in the Krishna-Godavari Basin, India, Mem. Geol. Soc. India 37 (1996) 285–295.
[2] E. Venkayya, Deccan Trap outliers of the Godavari districts, Proc. Indian Acad. Sci. 29 (1949) 431–441.
[3] E.H. Pascoe, A Manual of the Geology of India and Burma, vol. 3, Government of India, Calcutta, 1964, pp. 1345–2130.
[4] A.K. Baksi, G.R. Byerly, L. Chan, E. Farrar, Intracanyon flows in the Deccan province, India? Case history of the Rajahmundry Traps, Geology 22 (1994) 605–608.
[5] C. Hofmann, G. Féraud, V. Courtillot, $^{40}Ar/^{39}Ar$ dating of mineral separates and whole rocks from the Western Ghats lava pile: further constraints on duration and age of the Deccan traps, Earth Planet. Sci. Lett. 180 (2000) 13–27.
[6] V. Courtillot, G. Féraud, H. Maluski, D. Vandamme, M.G. Moreau, J. Besse, The Deccan flood basalts and the Cretaceous-Tertiary boundary, Nature 333 (1988) 843–846.
[7] D.S.N. Raju, C.N. Ravindran, A. Dave, B.C. Jaiprakash, J. Singh, K/T boundary events in the Cauvery and Krishna-Godavari basins and the age of Deccan volcanism, Geosci. J. 12 (1991) 177–190.
[8] A.N. Halkett, Mantle plumes and the sedimentary record: onshore-offshore India, Ph.D. dissertation, University of Cambridge, 2002, 223 pp.
[9] J.E. Beane, C.A. Turner, P.R. Hooper, K.V. Subbarao, J.N. Walsh, Stratigraphy, composition and form of the Deccan Basalts, Western Ghats, India, Bull. Volc. 48 (1986) 61–83.
[10] S.S. Sun, W.F. McDonough, Chemical and isotopic systematics of oceanic basalts: implications for mantle composition and processes, in: Magmatism in Ocean Basins, Geol. Soc. Spec. Publ., London, 1989, pp. 313–345.
[11] W.F. McDonough, S.S. Sun, The composition of the Earth, Chem. Geol. 120 (1995) 223–254.
[12] A. Baksi, The Rajahmundry Traps, Andhra Pradesh: Evaluation of their petrogenesis relative to the Deccan Traps, Proc. Indian Acad. Sci. 110 (2001) 397–407.
[13] P.K. Banerjee, N.C. Ghose, V. Ravikumar, S. Chacko, Petrography, geomagnetism, and rare-earth element abundances of the Rajahmundry lavas, eastern India, J. Southeast Asian Earth Sci. 13 (1996) 139–143.

[14] B.C. Jaiprakash, J. Singh, D.S.N. Raju, Foraminiferal events across K/T boundary and age of Deccan volcanism in Palakollu area, Krishna-Godavari Basin, India, J. Geol. Soc. India 41 (1993) 105–117.
[15] V.L.S. Bhimasankaram, Paleomagnetic directions of the Deccan Traps of Rajahmundry, Andhra Pradesh, India, Geophys. J. 9 (1965) 113–119.
[16] J. Singh, M.S. Bhalla, Preliminary paleomagnetic studies on igneous rocks of U.P., Andhra Pradesh and Mysore, Curr. Sci. 41 (1972) 92–94.
[17] D. Vandamme, V. Courtillot, Paleomagnetic constraints on the structure of the Deccan traps, Phys. Earth Planet. Inter. 74 (1992) 241–261.
[18] K.V. Subbarao, S. Pathak, Reversely magnetized flows, Rajahmundry, Andhra Pradesh, J. Geol. Soc. India 41 (1993) 71–72.
[19] N. Krishna Brahmam, Comment on the paper entitled 'Reversely magnetized flows, Rajahmundry, Andhra Pradesh' by K.V. Subbarao and S. Pathak, J. Geol. Soc. India 41 (1993) 561–562.
[20] D. Vandame, V. Courtillot, J. Besse, R. Montigny, Paleomagnetism and age determinations of the Deccan Traps (India): Results of a Nagpur-Bombay traverse and review of earlier work, Rev. Geophys. 29 (1991) 159–190.
[21] C.H. Lo, T.C. Onstott, Ar-39 recoil artifacts in chloritized biotite, Geochim. Cosmochim. Acta 53 (1989) 2697–2711.
[22] P.R. Renne, C.C. Swisher, A.L. Deino, D.B. Karner, T.L. Owens, D.J. DePaolo, Intercalibration of standards, absolute ages and uncertainties in $^{40}Ar/^{39}Ar$ dating, Chem. Geol. 145 (1998) 117–152.
[23] P.R. Renne, E.B. Norman, Determination of the half-life of ^{37}Ar by mass spectrometry, Phys. Rev. C 63 (2001) art. no. 047302.
[24] K. Min, R. Mundil, P.R. Renne, K.R. Ludwig, A test for systematic errors in $^{40}Ar/^{39}Ar$ geochronology through comparison with U-Pb analysis of a 1.1 Ga rhyolite, Geochim. Cosmochim. Acta 64 (2000) 73–98.
[25] R.P. Esser, W.C. McIntosh, M.T. Heizler, P.R. Kyle, Excess argon in melt inclusions in zero-age anorthoclase feldspar from Mt. Erebus, Antarctica, as revealed by the 40Ar/39Ar method, Geochim. Cosmochim. Acta 61 (1997) 3789–3801.
[26] S. Kelley, Excess argon in K-Ar and Ar-Ar geochronology, Chem. Geol. 188 (2002) 1–22.
[27] Z.X. Peng, J. Mahoney, P. Hooper, C. Harris, J. Beane, A role for lower continental crust in flood basalt genesis? Isotopic and incompatible element study of the lower six formations of the western Deccan Traps, Geochim. Cosmochim. Acta 59 (1994) 267–288.
[28] L. Melluso, L. Beccaluva, P. Brotzu, A. Grenanin, A.K. Gupta, L. Morbidelli, G. Traversa, Constraints on the mantle sources of the Deccan Traps from the petrology and geochemistry of the basalts of Gujarat State (Western India), J. Pet. 36 (1995) 1393–1432.
[29] Z.X. Peng, J.J. Mahoney, P.R. Hooper, J.D. Macdougall, P. Krishnamurthy, Basalts of the northeastern Deccan Traps, India: Isotopic and elemental geochemistry and relation to southwestern Deccan stratigraphy, J. Geophys. Res. 103 (1998) 29843–29865.
[30] S.Z. Bilgrami, A reconnaissance geological map of the eastern part of the Deccan Traps (Bidar-Nagpur), Mem. Geol. Soc. India 43 (1999) 219–232.
[31] J.J. Mahoney, H.C. Sheth, D. Chandrasekharam, Z.X. Peng, Geochemistry of flood basalts of the Toranmal section, Northern Deccan Traps, India: Implications for regional Deccan stratigraphy, J. Pet. 41 (2000) 1099–1120.
[32] P.C. Lightfoot, C.J. Hawkesworth, C.W. Devey, N.W. Rogers, P.W.C. Van Calsteren, Source and differentiation of Deccan Trap lavas: Implications of geochemical and mineral chemical variations, J. Pet. 31 (1990) 1165–1200.
[33] K.G. Cox, C.J. Hawkesworth, Geochemical stratigraphy of the Deccan Traps at Mahabaleshwar, Western Ghats, India, with implications for open system magmatic processes, J. Pet. 26 (1985) 355–377.
[34] T. Sano, T. Fujii, S.S. Deshmukh, T. Fukuoka, S. Aramaki, Differentiation processes of Deccan Trap basalts: Contribution from geochemistry and experimental petrology, J. Pet. 42 (2001) 2175–2195.
[35] P.C. Lightfoot, C.J. Hawkesworth, Origin of Deccan Trap lavas: Evidence from combined trace element and Sr-, Nd- and Pb isotope studies, Earth Planet. Sci. Lett. 91 (1988) 89–104.
[36] I. Kaneoka, H. Haramura, K-Ar ages of successive lava flows from the Deccan Traps, India, Earth Planet. Sci. Lett. 18 (1973) 229–236.
[37] C.J. Allègre, B. Dupre, P. Richard, D. Rousseau, C. Brooks, Subcontinental versus suboceanic mantle; II, Nd-Sr-Pb isotopic comparison of continental tholeiites with mid-ocean ridge tholeiites, and the structure of the continental lithosphere, Earth Planet. Sci. Lett. 57 (1982) 25–34.
[38] P.R. Hooper, The Columbia River Basalt, in: J.D. Macdougall (Ed.), Continental Flood Basalts, Kluwer, 1988, pp. 1–33.
[39] A.M. Ho, K.V. Cashman, Temperature constraints on the Ginkgo flow of the Columbia River Basalt Group, Geology 25 (1997) 403–406.
[40] S. Self, T. Thordarson, L. Keszthelyi, Emplacement of continental flood basalt lava flows, large igneous provinces, Geophys. Monogr. 100 (1997) 381–410.
[41] D.H. Elliot, T.H. Flemming, P.R. Kyle, K.A. Foland, Long-distance transport of magmas in the Jurassic Ferrar Large Igneous Province, Antarctica, Earth Planet. Sci. Lett. 167 (1999) 89–104.
[42] W.R.A. Baragar, R.E. Ernst, L. Hulbert, T. Peterson, Longitudinal petrochemical variation in the Mackenzie dyke swarm, Northwestern Canadian shield, J. Pet. 37 (1996) 317–359.
[43] J.S. Marsh, M.J. Mndaweni, Geochemical variations in a long Karoo dyke, Eastern Cape, S. Afr. J. Geol. 101 (1998) 119–222.
[44] M. Elburg, A. Goldberg, Age and geochemistry of Karoo dolerite dykes from northeast Botswana, J. Afr. Earth Sci. 31 (2000) 539–554.

[45] C.C. Swisher, L. Dingus, R.F. Butler, $^{40}Ar/^{39}Ar$ dating and magnetostratigraphic correlation of the terrestrial Cretaceous-Paleogene boundary and Puercan mammal age, hell-Creek-Tullock formations, eastern Montana, Can. J. Earth Sci. 30 (1993) 1981–1996.

[46] W.A. Berggren, D.V. Kent, C.C. Swisher III, M. Aubry, A revised Cenozoic geochronology and chronostratigraphy, SEPM Spec. Publ. 54 (1995) 129–212.

[47] R.H. Steiger, E. Jäger, Subcommission on geochronology: Convention on the use of decay constants in geo- and cosmochronology, Earth Planet. Sci. Lett. 36 (1977) 359–362.

[48] G. Audi, O. Bersillon, J. Blachot, A.H. Wapstra, The NUBASE evaluation of nuclear and decay properties, Nucl. Phys. A624 (1997) 1–124.